Reprinted from JOURNAL OF THE ELECTROCHEMICAL SOCIETY
Vol. 139, No. 8, August 1992
Printed in U.S.A.

The Use of a Scanning Tunneling Microscope to Estimate Film Thickness and Conductivity of an Electrochemically Produced Poly-1-aminoanthracene Film

Hongjun Yang,* Fu-Ren F. Fan, Shueh-Lin Yau, and Allen J. Bard**

Department of Chemistry and Biochemistry, The University of Texas at Austin, Austin, Texas 78712

ABSTRACT

An electronically conductive poly-1-aminoanthracene (PAA) film was prepared electrochemically on Pt, Au, and C substrates by cycling the potential between −0.40 and +0.80 V in MeCN/$TBAPF_6$ solutions. Adding pyridine to the solution resulted in a marked increase in the growth rate of the polymer film, as indicated by a large increase of faradaic current. A new scanning tunneling microscopy (STM) approach is also presented to determine film thickness and film conductivity through measuring the tip current *vs.* tip displacement. In this approach, the tip excursion between its initial contact with the polymer film and its contact with the Pt substrate is a measure of film thickness. A comparison of the STM current-displacement behavior in the poly-1-aminoanthracene film to that of a polypyrrole film relates to film conductivity. The PAA film was about an order of magnitude less conductive than polypyrrole.

We report here a preliminary study of the electrochemical preparation of an electronically conductive poly-1-aminoanthracene film. To our knowledge, this is the first report of the electrochemistry of 1-aminoanthracene. We also describe the application of the scanning tunneling microscope (STM) to measure the relative conductivity and local thickness of the film in air by current-tip displacement measurements.

Conducting polymers have attracted considerable research interest because of their novel electrical properties and their potential applications as new electronic materials[1,2]. For example, polyaniline-type films, formed by electrochemical polymerization of aniline and its derivatives, have been extensively studied[3,4]. Less attention has been paid to polynuclear aromatic amines. However, a few, *e.g.*, 1-naphthylamine, N,N-dimethyl-1-naphthylamine, and N,N,N′,N′-tetramethylnaphthidine in MeCN, methylene chloride, and dimethyl sulfoxide have been examined[5-12]. An electrochemical-chemical-electrochemical (ECE) type mechanism for the anodic oxidation of these compounds has been proposed. The polymer film formed by oxidation of the polynuclear aromatic amine, 1-pyrenamine, has been reported by Oyama and co-workers[13,14]. The conductivity of this poly(1-pyreneamine) film was low in the dry state, but the film was electroactive in aqueous and nonaqueous solutions.

Experimental

1-Aminoanthracene (90%, Aldrich Chemical Company, Inc., Milwaukee, WI) was purified by dissolving commercial aminoanthracene in MeCN. The insoluble impurities were filtered out, and the solvent was then evaporated on a Rotovap. The resultant solids were recrystallized twice from cyclohexane. The aminoanthracene crystals were dried in a vacuum oven at 60°C overnight. Tetra-n-butylammonium hexafluorophosphate, $TBAPF_6$ (SACHEM, Austin, TX), the supporting electrolyte, was recrystallized twice from ethanol and acetone. MeCN (0.004% water, Burdick & Jackson) was used as received, but *ca.* 0.5 g ICN Alumina N-Super 1 (ICN Biomedicals Inc., Costa Mesa, CA) was added to the solution for further drying. Other chemicals were reagent grade and were used as received.

A single-compartment three-electrode cell containing 10 ml of solution was used in the experiments. A silver wire was used as a quasi-reference electrode (AgQRE) and was isolated by a coarse glass frit. The working electrode was a platinum disk. For scanning electron microscope (SEM) examination, Pt and Au disk electrodes were prepared by sputtering the metals on glass slides. A Pt flag was used as the counterelectrode. All potentials reported here are referred to SCE after calibration of the AgQRE against the decamethylferrocene/decamethylferrocenium couple, with the potential of this couple taken as 0.12 V *vs.* SCE[15]. Before aminoanthracene was added to the solution, MeCN with supporting electrolyte, it was purged with argon for 10 min until the background voltammogram (checked by potential sweeps between 2.0 and −2.0 V) was flat. The solution was kept under an argon atmosphere during the experiment.

The STM has been described previously[16] and comprises a micrometer-driven differential spring assembly for sample movement and a piezoelectric tripod to control the displacement of the tip electrode. The feedback circuit for regulating the z-piezoelectric was not required in the present experiments, while a sample-and-hold circuit was used to control the tip excursions Δz. The bias voltage between the tip and sample was held constant while the *z*-voltage of the piezo was steadily increased to ramp the tip toward the sample. The tip was retracted from the sample as soon as the tip current was higher than a preset current of 30 nA. All the experiments were conducted in air. All the polymer films were emersed at their conducting state, approximately +1.0 V. Medium sharp STM tunneling probes were prepared by electrochemically etching 250 or 125 μm Pt/Ir wire. The STM *i vs.* Δz curves were reproducible at different locations for thin film samples (<500 Å), but on thicker layer samples they were less reproducible, presumably due to surface roughness. The initial vertical tip-to-sample distance was set at a position (z_0) which just gave detectable current (*ca.* 1 pA for our circuit). Each *i vs.* Δz curve is the average of several scans.

Results and Discussion

Electropolymerization of 1-aminoanthracene.—The electrochemical behavior of 1-aminoanthracene (AA) was examined by cyclic voltammetry (CV) in neutral MeCN (Fig. 1). In the first anodic scan at 0.2 V/s, only one peak was observed at 0.60 V *vs.* SCE, with no corresponding reversal peak in the cathodic scan, even at scan rates up to 500 V/s. However, several new peaks were observed in the reverse cathodic scan and the second anodic scan. Two pairs of well-defined peaks, II/VI and III/V, that represent two redox processes, appeared at less positive potentials. Peak VI merged with peak I, but at higher scan rates peak VI formed a distinct wave. Peaks III and V were broader than II and VI, and the peak currents of the III/V couple were lower than those of the II/VI couple. While these two couples have not yet been identified, this voltammogram is very similar to the CV of 1-naphthylamine. The electrode process of the latter was attributed to an ECE-type reaction pathway[5,6]. Radical cations of AA generated upon oxidation were completely consumed in a rapid following

* Electrochemical Society Student Member.
** Electrochemical Society Life Member.

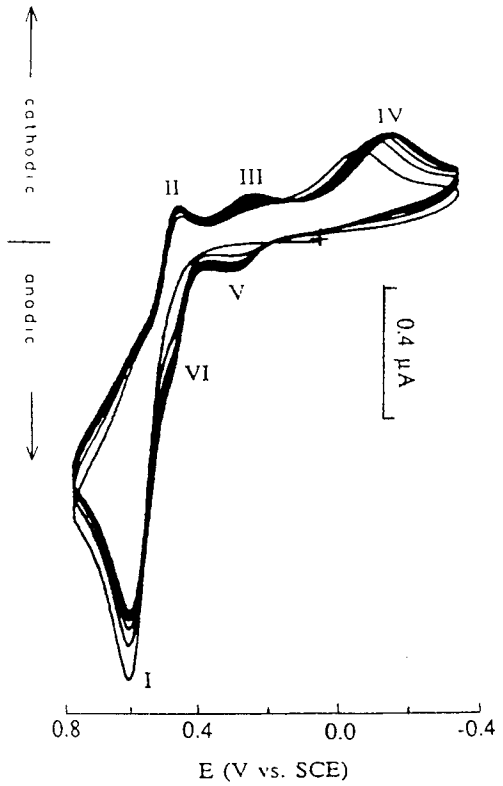

Fig. 1. Cyclic voltammogram of 1.45 mM l-aminoanthracene in 0.10M $TBAPF_6$/MeCN solution with 0.55 mm diam Pt disk at scan rate = 0.20 V/s.

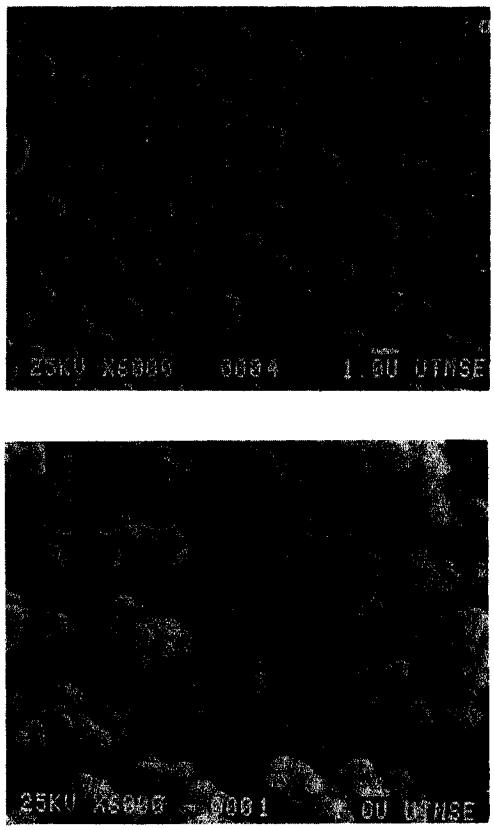

Fig. 2. Scanning electron micrographs of films obtained (a, top) under the conditions in Fig. 1; (b, bottom) under the conditions in Fig. 1, but in the presence of pyridine (1 mM).

chemical reaction. In this case, the most likely reaction, as with other amines, is dimerization of the cation radicals followed by deprotonation

$$ArNH_2 - e \rightleftarrows ArNH_2^+\cdot \quad [1]$$

$$2ArNH_2^+\cdot \rightleftarrows (ArNH)_2 + 2H^+ \quad [2]$$

$$(ArNH)_2 - ne \rightleftarrows (ArNH)_2^{n+} \quad [3]$$

The redox potentials of such dimers are generally less positive than those of monomers. Thus, these two pairs of peaks presumably represent two different dimerization products. Both C_4-C_4- and C_4-N-coupled dimers were proposed for 1-naphthylamine[5,6,8]. If analogous coupling occurs with AA, analogous head-to-tail, and tail-to-tail coupling *para* to the NH_2 group would yield 1 and 2

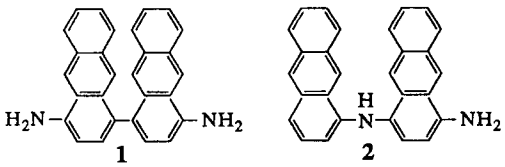

1

2

Peak IV corresponds to the reduction of solvated protons liberated in the above chemical reaction (Eq. 1-3). As potential cycling continued, peak I first decreased, then increased slowly while all of the other peaks increased slowly. When the Pt disk working electrode was removed from the cell, after cycling for one-half hour, and rinsed with acetone, a dark purple film was seen on the electrode surface. An SEM micrograph (Fig. 2) showed a thin, but quite uniform, film.

As mentioned above, the chemical step in Eq. 2 is associated with deprotonation. In neutral MeCN solution, the AA monomer can act as a base. Thus, during oxidation the concentration of protonated AA monomers increases in the vicinity of electrode surface and slows the reaction rates of dimerization[5]. When the base pyridine (Py) was added to the solution, the situation changed significantly. For a concentration of added pyridine about equal to that of the AA monomer, i_{pa} for peak *I* in the first scan was close to twice that obtained without added pyridine (Fig. 3). This implies that n in Eq. 3 should be 2 and the overall reaction, with $n_{app} = 2$, can be written as

$$2ArNH_2 + 2Py - 4e \rightarrow (ArNH)_2^{2+} + 2PyH^+ \quad [4]$$

compared to the overall reaction in the absence of pyridine ($n_{app} = 1$)

$$4ArNH_2 - 4e \rightarrow (ArNH)_2^{2+} + 2ArNH_3^+ \quad [5]$$

After several cycles, new waves appeared at *ca.* 0.75 V and all peaks grew rapidly (Fig. 3). This behavior has not been reported in other studies of amine electropolymerization.

To investigate further the dark purple polymer film that formed on the electrode surface, the electrode was removed from the cell, rinsed with acetone, and then put into an AA monomer-free solution. The cyclic voltammogram of the poly(1-aminoanthracene) (PAA) film-coated electrode in MeCN solution containing only supporting electrolyte is shown in Fig. 3b. The polymer film was electroactive at potentials more positive than 0.3 V. The anodic branch and cathodic branch were not symmetric. Figure 2b shows the morphology of this polymer film by SEM. The film formed in the presence of pyridine was thicker than that in Fig. 2a. Compared with a polyaniline film formed in aqueous solution, this film did not show a microfiber structure[17].

The same experiments were performed with Au and glassy carbon (GC) electrodes as substrates. The results were essentially the same, but the film was found to adhere best to a GC electrode. This can probably be attributed to the hydrophobicity of the film formed from a polynuclear amine. The behavior in the presence of 2,6-lutidine as a base was similar to that observed with pyridine. The polymer films were very stable in air and remained electroactive in the solution after repeated cycling. The presence of base appears to play an important role in the electropolymerization reaction.

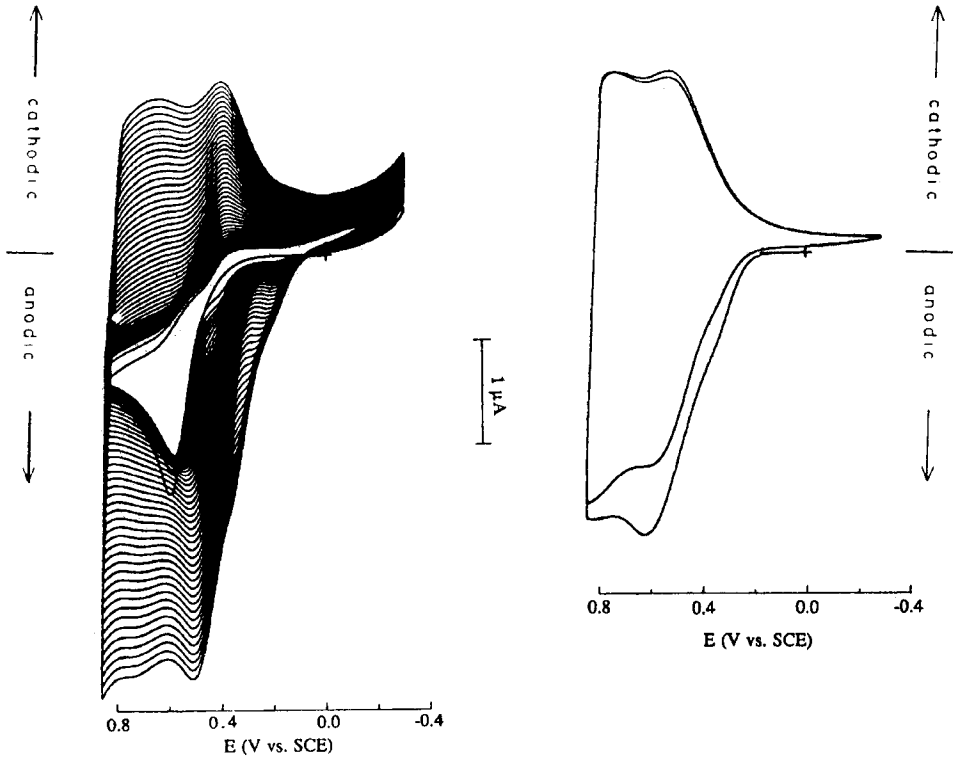

Fig. 3. (a, left) Cyclic voltammogram of 1.45 mM 1-aminoanthracene in 0.10M $TBAPF_6$/MeCN solution, in the presence of pyridine (1 mM); with 0.5 mm diam Pt disk at scan rate = 0.20 V/s. (b, right) Cyclic voltammogram of poly(1-aminoanthracene) film coated on a Pt electrode in 0.10M $TBAPF_6$/MeCN solution with 0.5 mm diam Pt disk at scan rate = 0.20 V/s.

STM characterization of poly-1-aminoanthracene film.— The principle of characterizing emersed soft conductive films in air with the STM is illustrated in Fig. 4. A tunneling current begins to flow when the tip approaches (~10 Å) the film (Fig. 4A). The current is governed by film resistance as it is driven through the polymer layer (Fig. 4B) and finally by tunneling directly to the substrate (Fig. 4C). Typical STM tip current (I) *vs.* tip displacement (Δz) curves

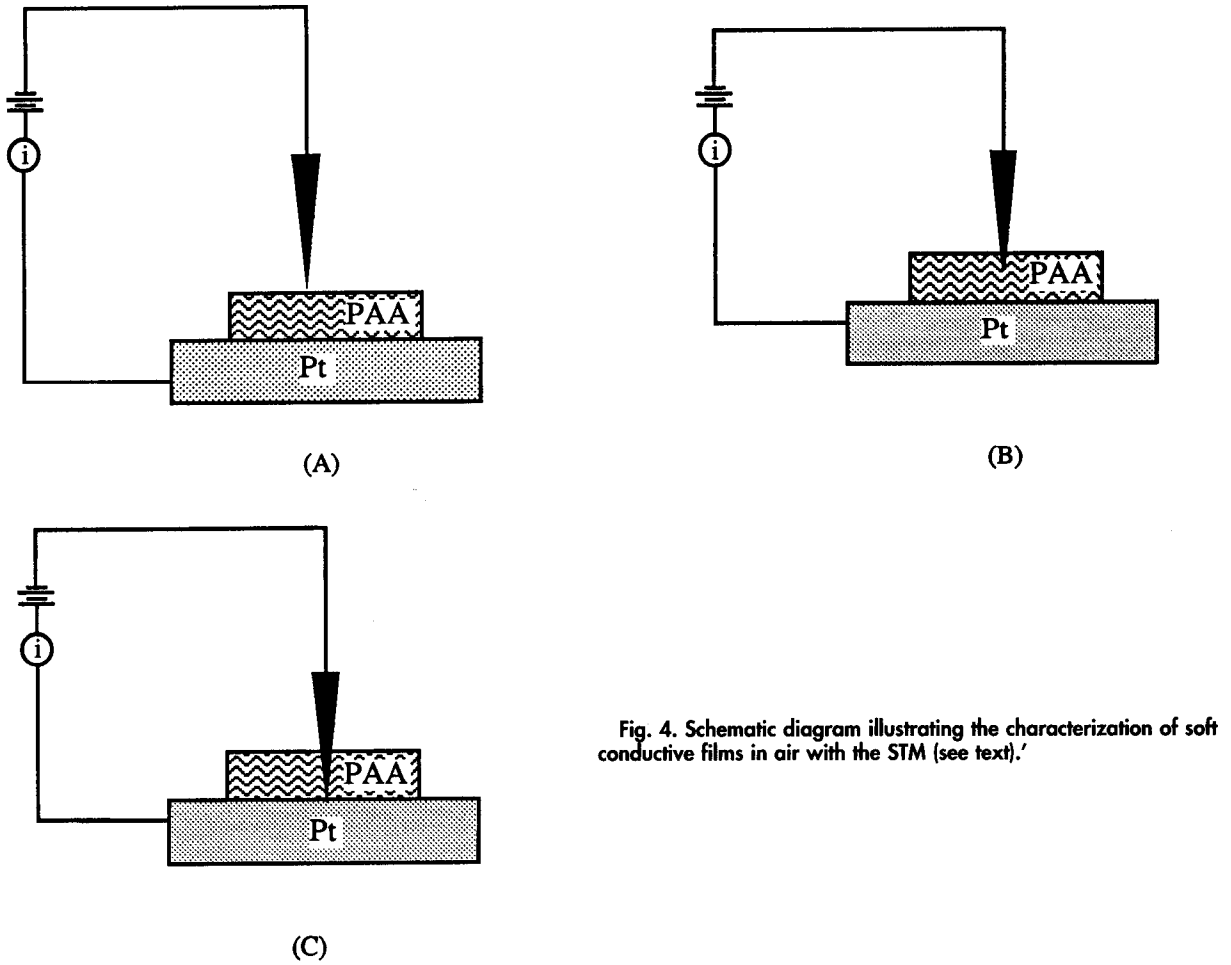

Fig. 4. Schematic diagram illustrating the characterization of soft conductive films in air with the STM (see text).

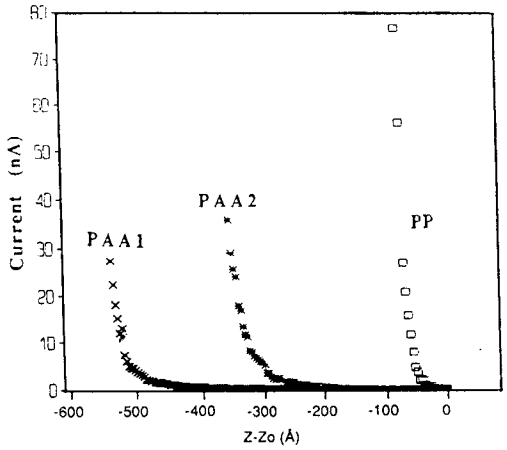

Fig. 5. Typical tip current *vs.* Δz (where $\Delta z = z - z_0$) curves taken in air for poly(1-aminoanthracene) films, PAA1 (~400 Å thick), PAA2 (~150 Å thick), and polypyrrole (PP). The reference *z* coordinate, z_0, was set at a position where 1 pA current was detected. The bias voltage of the sample was 1.55 V with respect to the tip.

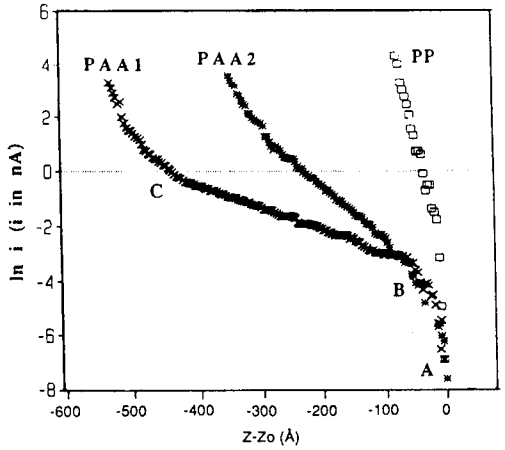

Fig. 6. Typical ln(i) *vs.* Δz for poly(1-aminoanthracene) films, PAA1, PAA2, and polypyrrole (PP) films from Fig. 5. Points B and C represent the transition from tunneling to contact and penetration of the film (contact with the Pt wsubstrate) for film PAA1.

taken in air with the STM tip initially above the film surface, are shown in Fig. 5. Note that the zero-point on these curves is arbitrary. The curves exhibit exponential-like behavior for PAA (thickness PAA1, ~400 Å, PAA2, ~150 Å) as well as for a polypyrrole (PP) film. When the data are plotted as ln (*i*) *vs.* Δz (Fig. 6), the curves show three almost linear segments with different slopes. This result indicates variations of conductivity with tip-to-sample distance. Consider the PAA1 curve obtained with the thicker PAA film. The steep increase of current for the AB regime represents the electron tunneling between tip and polymer before they are in physical contact. As the tip approaches the sample, point B marks contact; the current at point B represents the initial current reading after contact as governed by the film conductance. As the tip was further pushed into the film, the contact area increased and the tip to Pt substrate distance decreased, so that the current steadily increased, as shown by the linear BC segment of the curve. When the tip completely penetrated the film, came within tunneling distance, and finally contacted the Pt substrate, the current abruptly increased, as indicated by the larger slope beginning at point C.

For the thinner film, PAA2, the B inflection point is still discernible while the contact point C between the tip and the substrate is less well defined. The current increases more steeply after contact point B, as compared to the thicker film, PAA1, reflecting mainly the effect of the film thickness on its conductance. Apparently, at a bias voltage of 1.55 V the conductance changes from contact-limited to bulk-limited at a contact point B. For the more conductive polypyrrole film, the *i vs.* Δz curve does not have a clear C inflection point. The high conductance of the polypyrrole film, indicated by the very steep slope of the *i vs.* Δz curve after point B, tends to mask the inflection point C, making it somewhat ill defined, partly because of tip-substrate interactions, as discussed below. Nevertheless, the first inflection point which marked the point of physical contact can still be identified. The tunneling current immediately before the tip-substrate contact was about an order of magnitude higher for the polypyrrole film, which can be attributed to its higher conductivity. This method can be used to estimate the thickness of the film (the displacement between points B and C), as long as the slope of the ln (*i*) *vs.* Δz curve for the tip within the film is significantly less than that due to tunneling in air. Although the current after the tip contacts the film surface is a complicated function of Δz, because of changes in the tip-film contact area and possible distortion of the tip shape as it penetrates the film, this approach can still be used to estimate relative conductivity. In the present study, one can estimate from the tip current at the point of contact that the conductivity of the PAA film is approximately an order of magnitude lower than that of polypyrrole (assuming the same tip-contact area for these films). Thus, we roughly estimate a 2 s^{-1} cm^{-1} conductivity for the poly-1-aminoanthracene film. Further studies of this method of studying thin films with the STM and with the scanning electrochemical microscope are envisioned.

Acknowledgments

The support of this research by grants from the Office of Naval Research and the National Science Foundation is gratefully acknowledged.

Manuscript submitted Feb. 10, 1992; revised manuscript received April 20, 1992.

The University of Texas at Austin assisted in meeting the publication costs of this article.

REFERENCES

1. A. F. Diaz and J. Bargon, in *Handbook of Conducting Polymers*, T. A. Skotheim, Editor, Vol. 1, Marcel Dekker, Inc., New York (1986).
2. J. R. Ellis, in *Handbook of Conducting Polymers*, T. A. Skotheim, Editor, Vol. 1, Marcel Dekker, New York (1986).
3. E. M. Genies, A. Boyle, M. Lapkowski, and C. Tsintavis, *Synth. Met.*, **36**, 182 (1990).
4. W.-S. Huang, B. D. Humphrey, and A. G. MacDiarmid, *J. Chem. Soc., Faraday Trans. 1*, **82**, 2385 (1986).
5. N. Vettorazzi, J. J. Silber, and L. Sereno, *J. Electroanal. Chem.*, **125**, 459 (1981).
6. N. Vettorazzi, J. J. Silber, and L. Sereno, *ibid.*, **158**, 89 (1983).
7. E. M. Genies and M. Lapkowski, *Electrochim. Acta*, **32**, 1223 (1987).
8. J. M. Marioli, J. J. Silber, and L. Sereno, *ibid.*, **34**, 127 (1989).
9. A. H. Arevalo, H. Fernandez, J. J. Silber, and L. Sereno, *ibid.*, **35**, 741 (1990).
10. S. Daniele, P. Ugo, and G. A. Mazzocchin, *J. Electroanal. Chem.*, **267**, 129 (1989).
11. M. C. Miras, J. J. Silber, and L. Sereno, *ibid.*, **201**, 367 (1986).
12. M. C. Miras, J. J. Silber, and L. Sereno, *Electrochim. Acta*, **33**, 851 (1988).
13. N. Oyama, K. Hirabayashi, and T. Ohsaka, *Bull. Chem. Soc. Jpn.*, **59**, 2071 (1986).
14. T. Ohsaka, K. Hirabashi and N. Oyama, *ibid.*, **59**, 3423 (1986).
15. C. Zou and M. S. Wrighton, *J. Am. Chem. Soc.*, **112**, 7578 (1990).
16. F.-R. Fan and A. J. Bard, *J. Phys. Chem.*, **94**, 3761 (1990).
17. W.-S. Huang, B. D. Humphrey, and A. G. MacDiarmid, *J. Chem. Soc. Faraday Trans., 1*, **82**, 2385 (1986).